

THE QCD ANALYSIS OF THE COMBINED SET FOR THE F_3 STRUCTURE FUNCTION DATA BASED ON THE ANALYTIC APPROACH

A. V. Sidorov[†] and O. P. Solovtsova^{†,‡}

[†] *Joint Institute for Nuclear Research, 141980 Dubna, Russia*

[‡] *Gomel State Technical University, 246746 Gomel, Belarus*

Abstract

We apply analytic perturbation theory to the QCD analysis of the $xF_3(x, Q^2)$ structure function considering a combined set of deep inelastic scattering data presented by several collaborations, and extract values of the scale parameter Λ_{QCD} , the parameters of the form of the xF_3 structure function, and the x -shape of the higher twist contribution. We study the difference between the results obtained within the standard perturbative and analytic approaches in comparison with the experimental errors and state that the greatest difference occurs for large x .

Keywords: Quantum chromodynamics; deep inelastic scattering; structure functions, running coupling; higher twists.

PACS Nos.: 12.38.-t, 12.38.Cy, 12.39.Bx, 11.55.Hx, 11.55.Fv

1 Introduction

High-precision measurements of the deep inelastic scattering data open a possibility for testing new theoretical ideas in a wide kinematic range of x and Q^2 . In the present paper, we report the results of the application of the analytic approach in QCD [1, 2], called the analytic perturbation theory (APT), to the QCD analysis of the experimental data on the xF_3 structure function. In contrast to the perturbative running coupling which is spoiled by unphysical singularities in the infrared region at a scale $Q \sim \Lambda_{QCD}$, in the framework of the APT, the analytic coupling has no unphysical singularities. This fact stimulated applications of the APT and its modifications supporting correct analytic properties for various physical processes (see Refs. [3–11]), especially after the generalization of the APT method to the noninteger powers of the running coupling [12, 13].

This paper is a continuation of our previous analysis [14] of the xF_3 structure function data of the CCFR collaboration [15]. In the present analysis, we include in the consideration a set of various experimental xF_3 data: the CDHS [16], SCAT [17], BEBC-GARGAMELLE [18], BEBC-WA59 [19], NuTeV [20] and CHORUS [21]. Note that similar perturbative analysis was performed earlier in Ref. [22], but later the new data of the NuTeV and CHORUS collaborations were published, and we include these data in the present analysis. In accordance with the result of Ref. [16] concerning the disagreement of

CDHS data with perturbative QCD at small x , a cut $x \geq 0.35$ was applied to their data. The total number of experimental points is 289 and considerably exceeds the number of points considered before in Ref. [14]. It allows us to determine parameters of the form of the $x F_3$ structure function more precisely. The kinematic region of a combined set of data is $0.015 < x < 0.8$ and $0.5 \text{ GeV}^2 < Q^2 < 196 \text{ GeV}^2$. Thus, in addition to the previous analysis in Ref. [14] the kinematic region $0.5 \text{ GeV}^2 < Q^2 < 1.3 \text{ GeV}^2$ is now included. This region provides a possibility for more precise determination of the parameter Λ_{QCD} and the higher twist (HT) contribution. In order to achieve a more direct comparison of the perturbation theory (PT) and APT results for fit of a combine set of data, we do not introduce the normalization factors for the data of an individual collaboration.

In Sec. 2, we present the relevant theoretical expressions required for our analysis. In Sec. 3, we give the QCD fit results in the PT and APT approaches and compare the deviation of the APT results from the PT ones with the experimental uncertainties. Summarizing remarks are given in Sec. 4.

2 Basic relations

In this section, necessary expressions for our analysis are written and outline how we use them. We follow the well known approach based on the Jacobi polynomial expansion of structure functions. This method of solution of the Dokshitzer-Gribov-Lipatov-Altarelli-Parisi (DGLAP) evolution equation [23–26] was proposed in Refs. [27, 28] and developed for both unpolarized [29–36] and polarized cases [37–39]. The main formula of this method allows an approximate reconstruction of the structure function through a finite number of Mellin moments

$$xF_3^{N_{max}}(x, Q^2) = \frac{h(x)}{Q^2} + x^\alpha(1-x)^\beta \sum_{n=0}^{N_{max}} \Theta_n^{\alpha, \beta}(x) \sum_{j=0}^n c_j^{(n)}(\alpha, \beta) M_3(j+2, Q^2). \quad (1)$$

Here $h(x)/Q^2$ is the HT term, $\Theta_n^{\alpha, \beta}$ are the Jacobi polynomials, $c_j^{(n)}(\alpha, \beta)$ contain α - and β -dependent Euler Γ -functions where α, β are the Jacobi polynomial parameters, fixed by the minimization of the error in the reconstruction of the structure function.

The perturbative renormalization group Q^2 evolution of moments is well known (see, e.g., Refs. [40–42]) and in the leading order reads as

$$M_3^{pQCD}(N, Q^2) = \frac{[\alpha_s(Q^2)]^\nu}{[\alpha_s(Q_0^2)]^\nu} M_3(N, Q_0^2), \quad \nu(N) = \gamma_{NS}^{(0), N}/2\beta_0, \quad N = 2, 3, \dots, \quad (2)$$

where $\alpha_s(Q^2)$ is the QCD running coupling, $\gamma_{NS}^{(0), N}$ are the nonsinglet one-loop anomalous dimensions, $\beta_0 = 11 - 2n_f/3$ is the first coefficient of the renormalization group β -function, and n_f denotes the number of active flavors.

Unknown quantity $M_3(N, Q_0^2)$ in Eq. (2) could be parameterized as the Mellin moments of structure function xF_3 at some point, Q_0^2 :

$$M_3(N, Q_0^2) = \int_0^1 dx x^{N-2} x F_3(x, Q_0^2) = \int_0^1 dx x^{N-2} A x^a (1-x)^b (1+\gamma x), \quad N = 2, 3, \dots \quad (3)$$

The shape of the function $h(x)$ in Eq. (1) as well as the parameters A, a, b, γ in Eq. (3), and the scale parameter Λ_{QCD} are found by fit of a combined set of xF_3 -data [16–21]. The detailed description of the fitting procedure could be found in Ref. [43]. The target mass corrections are taken into account to the order $o(M_{nuc}^4/Q^4)$. We do not take into account the nuclear effect in the xF_3 (see estimations of this effect in Refs. [44, 45]).

In our analysis we use the analytic approach in QCD, the APT [1–3]. This approach gives the possibility of combining the renormalization group resummation with correct analytic properties in Q^2 -variable for physical quantities. It should be noted that the moments of the structure functions should be analytic functions in the complex Q^2 plane with a cut along the negative real axis (see Ref. [3] for more details), the ordinary PT description violates analytic properties. In the framework of the APT, the analytic coupling has no unphysical singularities and in the low- Q^2 domain, instead of rapidly changing Q^2 evolution, as occurs in the PT case, the APT approach leads to rather slowly changing functions (see, e.g., Refs. [9, 46]). In the asymptotic region of large Q^2 the APT and PT results coincide.

In the framework of the APT, expression (2) transforms as follows:

$$\mathcal{M}_3^{APT}(N, Q^2) = \frac{\mathcal{A}_\nu(Q^2)}{\mathcal{A}_\nu(Q_0^2)} \mathcal{M}_3(N, Q_0^2), \quad (4)$$

where the analytic function \mathcal{A}_ν is derived from the spectral representation and corresponds to the discontinuity of the ν th power of the PT running coupling

$$\mathcal{A}_\nu(Q^2) = \frac{1}{\pi} \int_0^\infty d\sigma \frac{\text{Im} \{ \alpha_{PT}^\nu(-\sigma - i\varepsilon) \}}{\sigma + Q^2}. \quad (5)$$

The mathematical tool for numerical calculations of \mathcal{A}_ν up to the four-loop level is given in Ref. [47]. Note that the function $\mathcal{A}_{\nu=1}(Q^2)$ defines the APT running coupling, $\alpha_{APT}(Q^2)$. In the leading order (LO), the ‘normalized’ analytic function $\bar{\mathcal{A}}_\nu = [\beta_0/(4\pi)]^\nu \mathcal{A}_\nu$ has rather a simple form (see Refs. [12, 48]) and can be written as

$$\bar{\mathcal{A}}_\nu^{LO}(Q^2) = [\bar{a}_{PT}^{LO}(Q^2)]^\nu - \frac{\text{Li}_\delta(t)}{\Gamma(\nu)}, \quad (6)$$

$$\text{Li}_\delta(t) = \sum_{k=1}^{\infty} \frac{t^k}{k^\delta}, \quad t = \frac{\Lambda^2}{Q^2}, \quad \delta = 1 - \nu,$$

where the ‘normalized’ PT running coupling $\bar{a}_{PT}^{LO}(Q^2) = \beta_0 \alpha_{PT}^{LO}(Q^2)/(4\pi) = 1/\ln(Q^2/\Lambda^2)$ and Li_δ is the polylogarithm function. For the case $\nu = 1$ expression (6) leads to the well-known APT result [1]

$$\alpha_{APT}^{LO}(Q^2) = \alpha_{PT}^{LO}(Q^2) + \frac{4\pi}{\beta_0} \frac{\Lambda^2}{\Lambda^2 - Q^2}. \quad (7)$$

One could see that at large Q^2 the second term in the R.H.S. of expression (7) is negative. It was confirmed qualitatively in the phenomenological analysis of the xF_3 data in Ref. [49]. It should be stressed that values of the QCD scale parameter Λ are different in the PT and

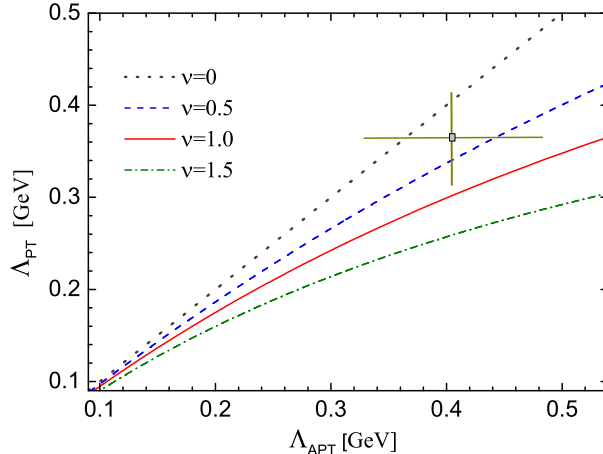


Figure 1: Values of Λ_{PT} vs. Λ_{APT} from Eq. (8) for different values of ν . The point corresponds to extracted values of Λ_{PT} and Λ_{APT} (with errors) presented in Table 1.

APT approaches. In order to illustrate this feature, in Fig. 1, we present the connection between the Λ_{PT} and the Λ_{APT} following from the condition

$$[\alpha_{\text{PT}}^{LO}(Q^2, \Lambda_{\text{PT}})]^\nu = \mathcal{A}_\nu^{LO}(Q^2, \Lambda_{\text{APT}}) \quad (8)$$

at different powers of ν . In this figure, the point marks the Λ_{PT} and Λ_{APT} values (see Table 1 below) with the corresponding experimental errors, which was found by fitting the $xF_3(x, Q^2)$ data.

3 Numerical results

The results of the leading order QCD fit of a combined set of xF_3 -data in the PT and APT approaches are presented in Table 1 and Figs. 1 – 6. In both cases the PT and APT are considered within the kinematic conditions $Q_0^2 = 3 \text{ GeV}^2$, $Q^2 > 0.5 \text{ GeV}^2$, for number of active flavours $n_f = 4$ and $N_{\text{Max}} = 11$. The values of A , a , b , γ , $h(x)$ and Λ are considered as free parameters.

As seen from Table 1, the analysis of a combined set of the xF_3 -data allows us to determine with good accuracy values of the parameter Λ_{QCD} . These values are different for the PT and APT cases, although consistent within errors. Errors in Table 1 correspond to $\Delta\chi^2 = 1$. It should be noted that due to the increased volume of experimental data, in the present analysis the errors for Λ_{PT} and Λ_{APT} are some times less than in our previous analysis of CCFR data [14] in which it was obtained $\Lambda_{\text{PT}} = 363 \pm 170 \text{ MeV}$ and $\Lambda_{\text{APT}} = 350 \pm 145 \text{ MeV}$. Also, one can see from Table 1 that the highest twist contribution is defined much more precisely than in our previous analysis [14] (for comparison see Fig. 4 in Ref. [14] and Fig. 6 below).

Let us turn now to Fig. 1, in which the extracted Λ -values is shown as a point with the corresponding experimental errors. One could see this point is in the region of small powers of ν , $\nu < 1$, which corresponds effectively to small numbers of the Mellin moments and, consequently, to small values of x .

Table 1: The results for the QCD leading order fit of a combined set on the xF_3 data in the standard PT and the APT approaches at $Q_0^2 = 3 \text{ GeV}^2$, $Q^2 > 0.5 \text{ GeV}^2$, $n_f = 4$, and $N_{Max} = 11$.

	PT	APT
A	3.75 ± 1.97	3.74 ± 0.64
α	0.65 ± 0.14	0.65 ± 0.05
β	3.62 ± 0.07	3.97 ± 0.04
γ	2.75 ± 2.33	3.56 ± 0.89
$\Lambda \text{ [MeV]}$	363 ± 49	407 ± 75
$\chi_{d.f.}^2$	1.80	1.83
x	$h(x) \text{ [GeV}^2\text{]}$	$h(x) \text{ [GeV}^2\text{]}$
$x < 0.02$	-0.053 ± 0.037	0.037 ± 0.015
$0.02 - 0.05$	-0.058 ± 0.030	-0.099 ± 0.019
$0.05 - 0.08$	-0.171 ± 0.038	-0.211 ± 0.027
$0.08 - 0.15$	-0.325 ± 0.050	-0.360 ± 0.035
$0.15 - 0.40$	-0.510 ± 0.048	-0.537 ± 0.056
$0.40 - 0.60$	-0.308 ± 0.085	-0.227 ± 0.064
$x > 0.60$	0.127 ± 0.053	0.181 ± 0.054

Figure 2 shows the xF_3 -shape obtained in the APT (solid line) and the PT (dotted line) cases. One can see that the result for the APT approach is slightly higher than for the PT one for small x , and less for large x .

Further, we will consider the difference between the PT and APT fit results in comparison with the experimental errors and will try to answer the question: In what kinematic areas the deviation goes beyond the experimental uncertainties of the APT-fit result?

In Fig. 3, we plot the difference in the x -shape of the xF_3 structure function

$$\Delta(xF_3) = xF_3^{PT}(x) - xF_3^{APT}(x) \quad (9)$$

in comparison with the experimental uncertainties for xF_3^{APT} at $Q_0^2 = 3 \text{ GeV}^2$. Gray color shows a corridor of experimental errors for xF_3^{APT} . As can be seen from Fig. 3, the difference $\Delta(xF_3)$ is beyond the experimental errors as at small $0.05 < x < 0.2$ as well at large values of a variable x , $x \gtrsim 0.4$. At large x values the deviation of the results of the PT from the APT exceeds several times the width of a corridor of experimental errors.

Figure 4 shows the difference between the moments in the PT and APT determined by using Eqs. (2) and (4), respectively,

$$\Delta M_3(N, Q^2) = M_3^{PT}(N, Q^2) - \mathcal{M}_3^{APT}(N, Q^2) \quad (10)$$

as a function of the number of the Mellin moments (including non integral value of N) in a wide range of $0.5 < N < 8$ at values $Q^2 = 0.5 \text{ GeV}^2$ (left panel) and $Q^2 = 5 \text{ GeV}^2$ (right panel). Comparing the results shown on the left and right panels in Fig. 4 one can see that in case of small Q^2 -values the difference ΔM_3 goes beyond experimental errors at $N \simeq 1$ and exceeds several times the width of this corridor of the experimental errors at $N \gtrsim 1.5$. For $Q^2 = 5 \text{ GeV}^2$ this effect is less pronounced.

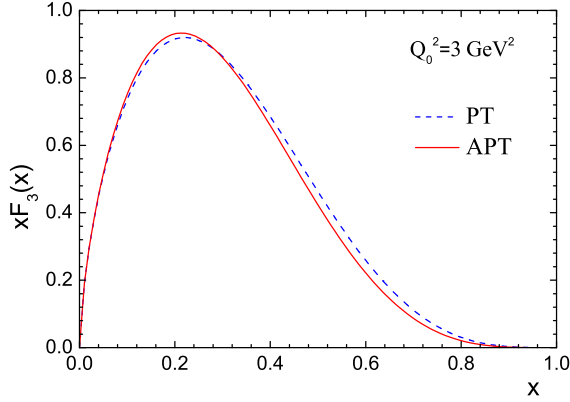


Figure 2: The x -behaviour of xF_3 obtained in the APT (solid line) and the PT (dashed line) at $Q_0^2 = 3 \text{ GeV}^2$.

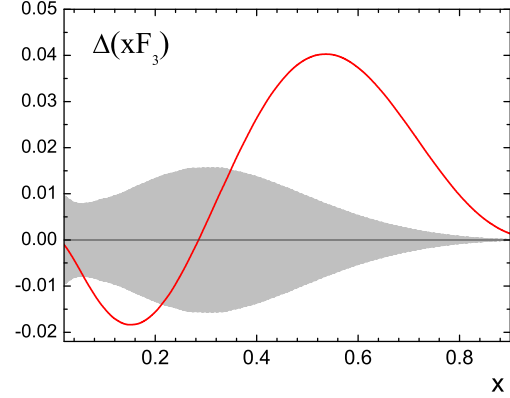


Figure 3: The difference $\Delta(xF_3)$ (solid line) from Eq. (9) in comparison with the experimental uncertainties of xF_3^{APT} (shaded area) at $Q_0^2 = 3 \text{ GeV}^2$.

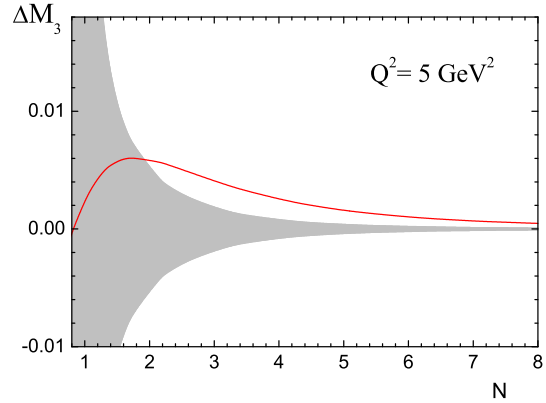
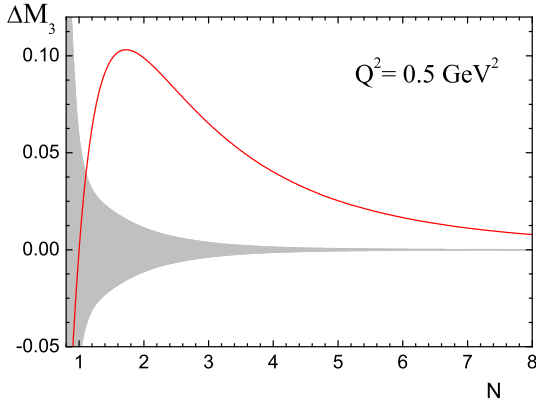


Figure 4: The difference $\Delta M_3(N, Q^2)$ (solid line) from Eq. (10) for $Q^2 = 0.5 \text{ GeV}^2$ (left panel) and $Q^2 = 5 \text{ GeV}^2$ (right panel) is shown as a function of a number of Mellin moment N . The shaded area shows the experimental uncertainties of $\mathcal{M}_3^{APT}(N, Q^2)$.

Let us consider the difference between the PT and APT approaches for the evolution factor, $E_\nu(Q^2, Q_0^2)$, which is given by $E_\nu^{PT} = [\alpha_s(Q^2)/\alpha_s(Q_0^2)]^\nu$ for the PT and $E_\nu^{APT} = \mathcal{A}_\nu(Q^2)/\mathcal{A}_\nu(Q_0^2)$ for the APT, see Eqs. (2) and (4), respectively. In this case we consider the quantity

$$\Delta_\nu(Q^2) = E_\nu^{PT}(Q^2) - E_\nu^{APT}(Q^2) \quad (11)$$

as a function of noninteger ν at $Q_0^2 = 3 \text{ GeV}^2$. We present $\Delta_\nu(Q^2)$ in Fig. 5 for values $Q^2 = 0.5 \text{ GeV}^2$ (left panel) and $Q^2 = 5 \text{ GeV}^2$ (right panel). The shaded area shows the experimental uncertainties of $E_\nu^{APT}(Q^2)$. This uncertainty is related with errors of the only parameter Λ_{APT} (see Table 1).

In general, the consideration of Figs. 2 – 5 shows that the greatest difference between the results of the PT and APT approaches should be expected at low Q^2 and large numbers of Mellin moments N , which corresponds to large values of the variable x .

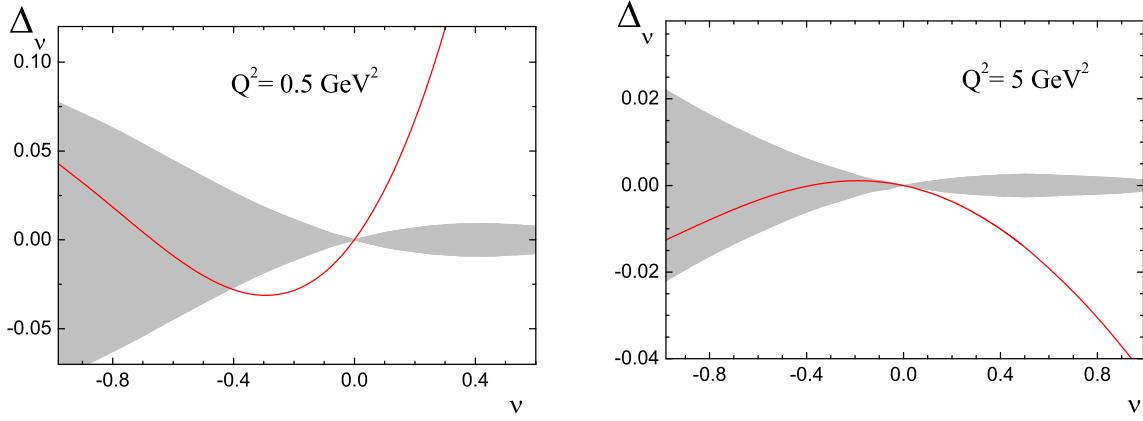


Figure 5: The quantity Δ_ν from Eq. (11) for $Q^2 = 0.5 \text{ GeV}^2$ (left panel) and $Q^2 = 5 \text{ GeV}^2$ (right panel) compared with the experimental uncertainties of the APT evolution factor E_ν^{APT} (shaded area) at $Q_0^2 = 3 \text{ GeV}^2$.

Finally, in Fig. 6 the results of the x dependence for the higher twists contribution in the PT and APT approaches are presented. They are in qualitative agreement with each other. Our results are in qualitative agreement with the results of other papers on extraction of a contribution of the highest twists in the structure function xF_3 [35, 36, 44, 45]. Accuracy of definition of the function $h(x)$ considerably (a few times) increased, in comparison with our result [14] of the analysis of CCFR data. In our previous analysis we noticed that $h^{APT}(x) > h^{PT}(x)$ for $x > 0.3$ [14]. Here we confirm this relation with higher accuracy. It should be noted that this inequality is in qualitative agreement with the result obtained for the shape of the HT contribution for the non-singlet approach for the F_2 structure function [50]. One could see from Fig. 6 that the opposite inequality takes place for small values $x < 0.3$: $h^{APT}(x) < h^{PT}(x)$.

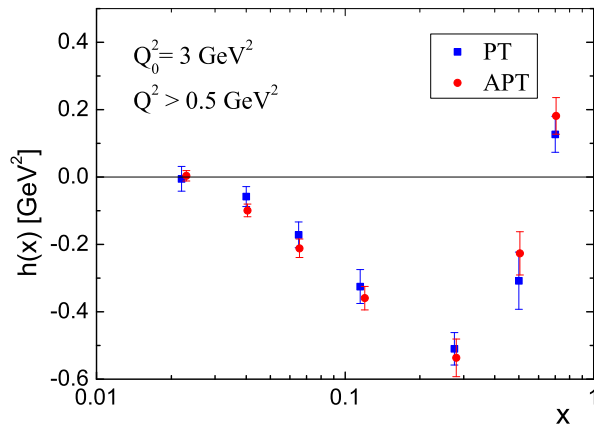


Figure 6: Higher twist contribution resulting from the leading order QCD analysis of the xF_3 combined data for the PT (squares) and APT (circles) approaches.

4 Conclusions

This work could be considered as a continuation of our work [14], in which for the first time the APT approach was applied to the analysis of the xF_3 structure function data. In this work, we used a combined set of data presented by various collaborations. Thus, a new kinematic region of experimental data $0.5 \text{ GeV}^2 < Q^2 < 1.3 \text{ GeV}^2$ was included in analysis. As a result, the QCD scale parameter Λ , the parameters of the shape of the structure function and the x -shape of the higher twist contribution were defined with high accuracy. The shape of this contribution is in qualitative agreement with the results of the previous analysis of the xF_3 structure function data. We compared the difference of the results of the PT and APT analysis with the corridor of experimental uncertainties. We revealed that the most essential difference in the PT and APT results should be expected for small Q^2 and large numbers of Mellin moments, which approximately corresponds to large values of a variable x .

Acknowledgments

It is a pleasure for the authors to thank S. V. Mikhailov, O. V. Teryaev and V. L. Khandramai for interest in this work and helpful discussions.

This research was supported by the JINR-BelRFFR grant F14D-007, the Heisenberg-Landau Program 2014, JINR-Bulgaria Collaborative Grant, and by the RFBR Grants (Nos. 12-02-00613, 13-02-01005 and 14-01-00647).

References

- [1] D. V. Shirkov and I. L. Solovtsov, *Phys. Rev. Lett.* **79**, 1209 (1997).
- [2] K. A. Milton and I. L. Solovtsov, *Phys. Rev. D* **55**, 5295 (1997).
- [3] D. V. Shirkov and I. L. Solovtsov, *Theor. Math. Phys.* **150**, 132 (2007).
- [4] M. Baldicchi, A. V. Nesterenko, G. M. Prosperi, D. V. Shirkov, and C. Simolo, *Phys. Rev. Lett.* **99**, 242001 (2007).
- [5] A. P. Bakulev, *Phys. Part. Nucl.* **40**, 715 (2009).
- [6] G. Cvetič, A. Y. Illarionov, B. A. Kniehl, and A. V. Kotikov, *Phys. Lett. B* **679**, 350 (2009).
- [7] G. Cvetič and A. V. Kotikov, *J. Phys. G* **39**, 065005 (2012).
- [8] G. Cvetič and C. Villavicencio, *Phys. Rev. D* **86**, 116001 (2012).
- [9] V. L. Khandramai, R. S. Pasechnik, D. V. Shirkov, O. P. Solovtsova, and O. V. Teryaev, *Phys. Lett. B* **706**, 340 (2012).
- [10] C. Ayala and G. Cvetič, *Phys. Rev. D* **87**, 054008 (2013).
- [11] P. Allendes, C. Ayala, and G. Cvetič, *Phys. Rev. D* **89**, 054016 (2014).
- [12] A. P. Bakulev, S. V. Mikhailov, and N. G. Stefanis, *Phys. Rev. D* **72**, 074014 (2005); *Erratum: ibid.* **72**, 119908(E) (2005).
- [13] A. P. Bakulev, S. V. Mikhailov, and N. G. Stefanis, *Phys. Rev. D* **75**, 056005 (2007); *Erratum: ibid.* **77**, 079901(E) (2008).

- [14] A. V. Sidorov and O. P. Solovtsova, *Nonlin. Phenom. Complex Syst.* **16**, 397 (2013) [arXiv:1312.3082 [hep-ph]].
- [15] W. G. Seligman *et al.*, *Phys. Rev. Lett.* **79**, 1213 (1997).
- [16] J. P. Berge *et al.*, *Z. Phys. C* **49**, 187 (1991).
- [17] V. V. Ammosov *et al.*, IHEP Preprint No. 87-081, 1987, 19 p.
- [18] P. C. Bosetti *et al.*, *Nucl. Phys. B* **203**, 362 (1982).
- [19] K. Varvell *et al.*, *Z. Phys. C* **36**, 1 (1987).
- [20] M. Tzanov *et al.*, *Phys. Rev. D* **74**, 012008 (2006).
- [21] G. Onengut *et al.*, *Phys. Lett. B* **632**, 65 (2006).
- [22] A. V. Sidorov, *JINR Rapid Commun.* **80**, 11 (1996) [hep-ph/9609345].
- [23] V. N. Gribov and L. N. Lipatov, *Sov. J. Nucl. Phys.* **15** 438, (1972).
- [24] V. N. Gribov and L. N. Lipatov, *Sov. J. Nucl. Phys.* **15**, 675 (1972).
- [25] G. Altarelli and G. Parisi, *Nucl. Phys. B* **126** (1977) 298.
- [26] Yu. L. Dokshitzer, *Sov. Phys. JETP* **46**, 641 (1977).
- [27] G. Parisi and N. Surlas, *Nucl. Phys. B* **151**, 421 (1979).
- [28] I. S. Barker, C. B. Langensiepen, and G. Shaw, *Nucl. Phys. B* **86**, 61 (1981).
- [29] V. G. Krivokhizhin *et al.*, *Z. Phys. C* **36**, 51 (1987).
- [30] V. G. Krivokhizhin *et al.*, *Z. Phys. C* **48**, 347 (1990).
- [31] A. Benvenuti *et al.*, *Phys. Lett. B* **195**, 97 (1987).
- [32] A. Benvenuti *et al.*, *Phys. Lett. B* **223**, 490 (1989).
- [33] A. V. Kotikov, G. Parente, and J. Sanchez-Guillen, *Z. Phys. C* **58**, 465 (1993).
- [34] A. L. Kataev and A. V. Sidorov, *Phys. Lett. B* **331**, 179 (1994).
- [35] A. V. Sidorov, *Phys. Lett. B* **389**, 379 (1996).
- [36] A. L. Kataev *et al.*, *Phys. Lett. B* **388**, 179 (1996).
- [37] E. Leader, A. V. Sidorov, and D. B. Stamenov, *Int. J. Mod. Phys. A* **13**, 5573 (1998).
- [38] E. Leader, A. V. Sidorov, and D. B. Stamenov, *Phys. Rev. D* **58**, 114028 (1998).
- [39] C. Bourrely *et al.*, *Phys. Lett. B* **442**, 479 (1998).
- [40] A. J. Buras, *Rev. Mod. Phys.* **52**, 199 (1980).
- [41] V. G. Krivokhizhin and A. V. Kotikov, *Phys. Part. Nucl.* **40**, 1059 (2009).
- [42] F. J. Yndurain, *The Theory of Quark and Gluon Interactions*, 4th ed. (Springer, 2006).
- [43] A. L. Kataev *et al.*, *Phys. Lett. B* **417**, 374 (1998).
- [44] M. V. Tokarev and A. V. Sidorov, *Nuovo Cim. A* **110**, 1401 (1997).
- [45] S. A. Kulagin and A. V. Sidorov, *Eur. Phys. J. A* **9**, 261 (2000).
- [46] K. A. Milton, I. L. Solovtsov, and O. P. Solovtsova, *Phys. Rev. D* **60**, 016001 (2001).
- [47] A. P. Bakulev and V. L. Khandramai, *Comput. Phys. Commun.* **184**, 183 (2013).
- [48] N. G. Stefanis, *Phys. Part. Nucl.* **44**, 494 (2013) [arXiv:0902.4805 [hep-ph]].
- [49] A. V. Sidorov, *Nuovo Cim. A* **112**, 1527 (1999).
- [50] A. V. Kotikov, V. G. Krivokhizhin, and B. G. Shaikhatdenov, *Phys. Atom. Nucl.* **75**, 507 (2012).